Interaction Between Electromagnetic Field and Human Body for Dual Band Balanced Antenna Using Hybrid Computational Method

A. G. Alhaddad[#1], K. N. Ramli[#2], R. A. Abd-Alhameed[#3], and D-W. Zhou[#*4]

[#]*Mobile & Satellite Communications Research Centre, School of Engineering, University of Bradford, Bradford, West Yorkshire, United Kingdom, BD7 1DP*

[*]*Pace plc, Victoria Road, Saltaire, Bradford, UK*

***Abstract*—This paper describes a hybrid computational method which efficiently models the interaction between a small antenna placed in proximity with the human body. Results for several test cases of placed in different locations on the body are presented and discussed. The near and far fields were incorporated into the study to provide a full understanding of the impact on human tissue. The cumulative distribution function of the radiation efficiency and absorbed power is also provided. The antennas are assumed to be operating over the 2.4 GHz and 5.2 GHz WLAN frequencies.**

I. Introduction

In wireless communications the finite difference time domain (FDTD) method has become very well established as a both as a design and general analytical tool due to its comparative simplicity, robustness, and capability for handling inhomegeneity within volumetric complexity [1][2]. The introduction, by Taflove, of the total-scattered field formulation provided a major step forward in practical implementation [2], allowing algorithms to be implemented using incident plane waves from arbitrary directions. The computational FDTD domain is discretised into a number of cells which are scaled as a fraction of the wavelength. The associated time step must be kept small during the simulation to satisfy the Courant-Freiderichs stability criterion [2][3]. An absorbing boundary condition (ABC) must be applied to the outer boundary of the FDTD space to obtain the necessary spatial resolution to represent electromagnetic wave interactions in unbounded regions – i.e. to simulate the extension of the finite lattice to infinity. The ABC should be able to absorb the outwardly travelling waves with an extremely low reflection. The perfectly matched layer introduced by Berenger [4] allows boundary reflections better than -80 dB to be realized. FDTD is currently the most widely used method for numerical dosimetry, particularly for the field analysis required to estimate mobile handset radiation effect on the human body [5-9].

This paper presents a hybrid method to model the human body interaction with a dual band balanced antenna structure covering the 2.4 GHz and 5.2 GHz bands. The near and far field performance of the antenna is investigated, with the antenna mounted on several locations of the human body. The radiated and absorbed power distributions are computed for the antenna in the various locations, and with different polarizations. From this we may infer the radiation efficiency of the balanced antenna operating in proximity to the human body; the cumulative distribution function (CDF) of the radiation efficiency for these locations is also evaluated.

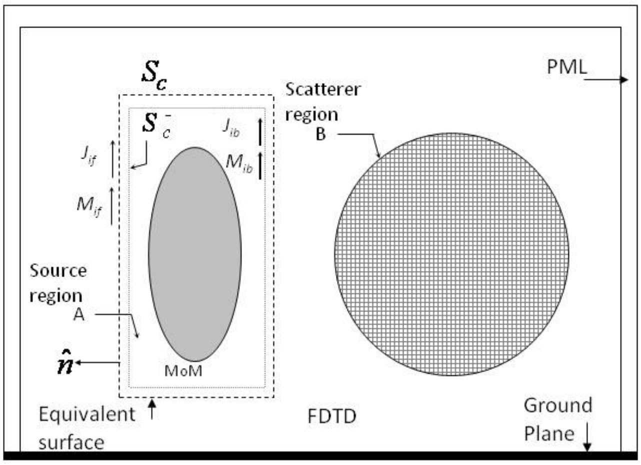

Figure 1: Hybrid MoM/FDTD configuration for the single source and scatterer geometries

II. Theoretical Formulation

Consider the electromagnetic geometry indicated in Fig. 1. This shows two regions, one representing the source region **A**, and the other the scatterer **B**. The source region is bounded by a closed Huygens surface S_c. The method starts by computing the fields due to the real currents of the source region (previously evaluated from the internal excitation) on the surface S_c, excluding the scatterer region **B**. These fields are computed by applying Galerkin's method with set of variable polynomial basis functions [10].

The equivalent surface currents on the surface S_c represent the outward travelling wave-fields from the source to the scatterer, due to the fields of the source region **A**, these may be written as:

$$\boldsymbol{J}_{if} = \boldsymbol{n} \times \boldsymbol{H}_{if} \quad (1)$$
$$\boldsymbol{M}_{if} = \boldsymbol{E}_{if} \times \boldsymbol{n} \quad (2)$$

where $\boldsymbol{n}$ is the outwardly directed unit normal to the surface from the source region. $\boldsymbol{H}_{if}$ and $\boldsymbol{E}_{if}$ are the forward scattered fields from the source region **A** on the equivalent surface S_c. $\boldsymbol{J}_{if}$ and $\boldsymbol{M}_{if}$ are the equivalent electric and magnetic source currents on the surface S_c. Thus these currents are treated as the source in the FDTD domain, propagating fields to the scatterer by using the $\boldsymbol{E}$ and $\boldsymbol{H}$ curl equations as follows:

$$\nabla \times \boldsymbol{E} = -\partial_t \boldsymbol{B} - \boldsymbol{M}_{if} \quad (3)$$
$$\nabla \times \boldsymbol{H} = \partial_t \boldsymbol{D} + \boldsymbol{J}_{if} \quad (4)$$

The FDTD updating equations for the field components are expanded with a three-dimensional modified total/scattered FDTD formulation for the special components on the Huygens' surface, while the rest of the problem space field components follow the normal updating equations.

The back-scattered fields were computed by FDTD at S_C^- (the closed surface interior to the surface S_c and bounding the region **A**). This surface is closed in the scattered field region, so that the calculated surface currents are due the scattered field only. The equivalent surface currents due to these fields, representing an additional source to the MoM domain (region **A**), are given by:

$$\boldsymbol{J}_{ib} = \boldsymbol{H}_{ib} \times \boldsymbol{n} \quad (5)$$
$$\boldsymbol{M}_{ib} = \boldsymbol{n} \times \boldsymbol{E}_{ib} \quad (6)$$

where $\boldsymbol{H}_{ib}$ and $\boldsymbol{E}_{ib}$ are the back-scattered fields computed at S_C^-. Note that $\boldsymbol{n}$ is as above, directed outwards from the source region. $\boldsymbol{J}_{ib}$ and $\boldsymbol{M}_{ib}$ are the electric and magnetic equivalent surface currents at S_C^-. Now, the voltage back scattered (the excitation for the MoM) on the source region can be evaluated using either of the following equations, defined by reciprocity theorem in the same way as in [10]:

$$\mathbf{V}_b = \langle \boldsymbol{J}_{ib} \cdot \boldsymbol{E}_{ms} - \boldsymbol{M}_{ib} \cdot \boldsymbol{H}_{ms}, d\boldsymbol{S}_C^- \rangle = \iint_{S_C^-} dS_C^- (\boldsymbol{J}_{ib} \cdot \boldsymbol{E}_{ms} - \boldsymbol{M}_{ib} \cdot \boldsymbol{H}_{ms}) \quad (7)$$

where

$$\boldsymbol{E}_{ib} = -j\omega \boldsymbol{A}(\boldsymbol{r}) - \nabla V(\boldsymbol{r}) - \frac{1}{\epsilon} \nabla \times \boldsymbol{F}(\boldsymbol{r})$$

$$\boldsymbol{A}(\boldsymbol{r}) = \mu \iint_{S_C^-} dS_C^- \{\boldsymbol{J}_{ib} G(\boldsymbol{r}, \boldsymbol{r}')\}$$

$$V(\boldsymbol{r}) = \frac{-j}{\omega\epsilon} \iint_{S_C^-} dS_C^- \{\nabla'_S \cdot \boldsymbol{J}_{ib} G(\boldsymbol{r}, \boldsymbol{r}')\}$$

$$\boldsymbol{F}(\boldsymbol{r}) = \epsilon \iint_{S_C^-} dS_C^- \{\boldsymbol{M}_{ib} G(\boldsymbol{r}, \boldsymbol{r}')\}$$

$G(\boldsymbol{r}, \boldsymbol{r}')$ is the free space green function. The vectors $\boldsymbol{r}$ and $\boldsymbol{r}'$ apply to the source and observation points respectively and S_a is the conducting surface area of the structure within region A. $\boldsymbol{J}_{ms}$ is the electric test function used on the wire. $\boldsymbol{E}_{ms}$ and $\boldsymbol{H}_{ms}$ are the electric and magnetic fields respectively for the test function $\boldsymbol{J}_{ms}$.

Equation (7) explicitly requires a double integral to evaluate $\boldsymbol{E}_{ib}$ and integrate over the surface on the antenna; assuming that the FDTD discretisation is very small compared to the operating wavelength. In this case Equation (7) can be reduced by ignoring the surface integral and evaluating the voltage back-scattered corresponding to the centre of the cell surface, by a summation over grid cell surfaces, to get the following equation for the hybrid MoM/FDTD case:

$$\mathbf{V}_b = \sum_{k=1}^{n_{S_C^-}} \Big(\boldsymbol{J}_{ib_k} \cdot \boldsymbol{E}_{ms}(\boldsymbol{r}_k, \boldsymbol{r}') - \boldsymbol{M}_{ib_k} \cdot \boldsymbol{H}_{ms}(\boldsymbol{r}_k, \boldsymbol{r}') \Big) a_k \quad (8)$$

where $\boldsymbol{r}_k$ is the position vector of the centre of the cell surface and a_k is the surface area of the cell surface. Therefore $\boldsymbol{J}_{ib_k}$ and $\boldsymbol{M}_{ib_k}$ are considered to be the equivalent surface currents at the centre of the surface cell n. Since the excitation voltages are known, the MoM can be executed to compute the new currents and the procedure can be repeated until the steady state solution is reached.

III. The Antenna

The antenna adopted in this study has been previously described by the authors in [11]. The antenna structure is a compact balanced dual band device, constructed by folding a thin strip planar dipole with an extra arm on each proposed monopole. The balanced design is intended to reduce the current flow on the conducting surface of the user terminal chassis. As a result the antenna has good efficiency, and maintains performance when held in proximity with the human body. This particular device was designed for short range WLAN communications operating in the 2.4 GHz (2.4-2.4835 GHz) and 5 GHz (5.15-5.35 GHz & 5.650-5.925 GHz) bands.

IV. Hybrid Model Method

This process begins by introducing a Huygens' surface around the balanced antenna. The equivalent electric and magnetic source on the Huygens' surface are produced at each time step from the electric and magnetic fields created by the antenna in free space using NEC [12]. This field data is used as an input source for the FDTD code. The Huygens' box is set as shown in Fig. 2, with volume of 30×24×54 FDTD cells. The FDTD method is applied over the entire computational domain. The equivalence principle is carried out in 3D by applying the hybrid electromagnetic method described in [13] with cell size dx=dy=dz= 6.0mm, and time step dt=5ps. A 6 cell PML is used to terminate the FDTD space, and the distance between the antenna and face of the box will be set to

2 cells. The human body model used in this study is known as the "Visible Man", the tissue-classified numerical model for which was developed at Brooks Air Force Base, San Antonio, TX [14].

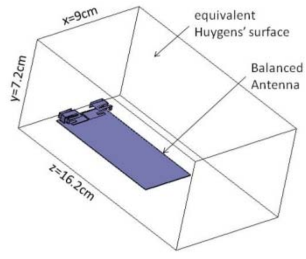

Figure 2: The balanced antenna with the equivalent Huygens box

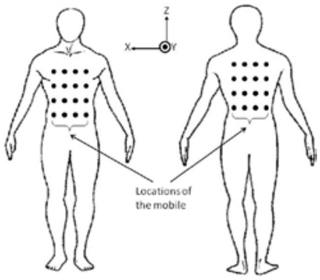

Figure 3: Human body model and the balanced antenna locations

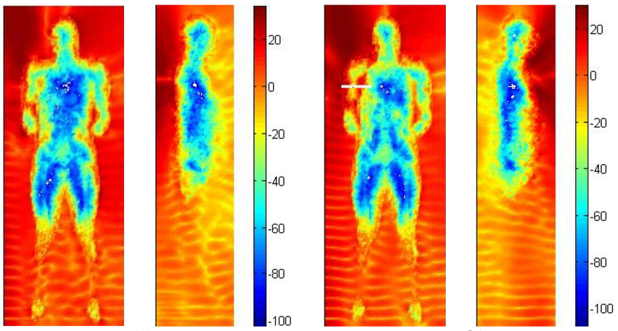

(a) (b)

Figure 4: Total electric field (dB) distributions when the mobile located in horizontal position, (a) Back Location,(b) Front Location

A. *Near field and Far field*

In order to investigate the performance of the antenna in proximity to the human body, the near and far field radiation of the antenna for different locations has been considered, as illustrated in Fig. 3. A total of 32 locations were investigated; 16 locations on the back, and 16 on the front, were taken. Due to the electric field distribution of these points being quite similar to each other, only one position for each case was demonstrated. Fig. 4 illustrates the electric field distribution in the neighborhood, and inside the human body, for the central y-z and x-y planes (dB scale) for the vertically polarized antenna position. Further simulations were performed on the radiation performance using the same antenna locations, but with different polarizations, these were found comparable to the other polarization.

The results of the investigation were conclusive, and made clear that regardless any changes in the polarization, the electric field distribution was almost the same when the mobile positions were changed. Again, as one may expect with the electric field distribution of these points being quite similar to each other, only one position for each case was demonstrated. Fig. 4 clearly illustrates the gulf between the two types of position: i.e. facing the human tissue (and its surrounding area), and that facing away. When the antenna is very close to the human tissue, the surrounded fields are much stronger, and this is clearly indicated in the figures.

Fig. 5 illustrates the far field components of the cases under investigation, the fields for y-z and x-y planes are normalized to one 1 watt input power. From the pattern variations it is clearly evident that the fields were considerably stronger in the direction directly facing the normal axis of the handset antenna, and consequently away from the human tissue.

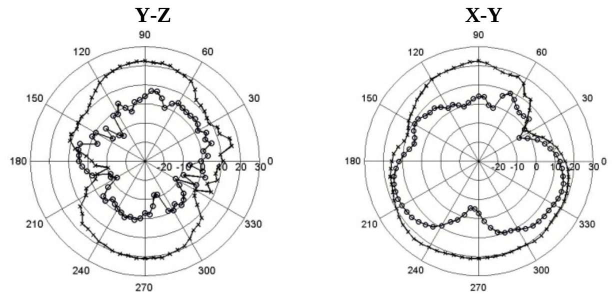

(a)

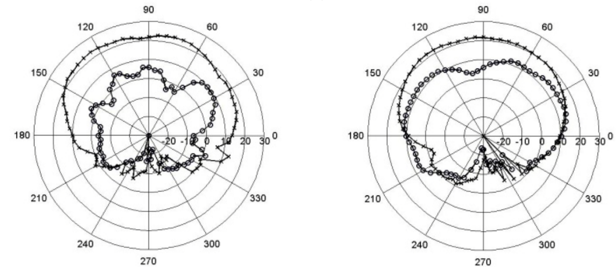

(b)

Figure 5: The far field patterns at 2.45 GHz yz, xz and xy planes; for vertical polarization (a) Back Location,(b) Front Location; where 'o-o-o' computed E_θ and 'x-x-x' computed E_ϕ.

Consequently, it is no surprise to notice the reduced field magnitudes caused by the tailing effect of the human body falling approximately between 20 dB and 25 dB. However it should be noted that for horizontal polarization the field distribution was quite similar to the vertical one in both manifestation and impact and thus are not presented here.

B. *Cumulative Distribution Function of the Radiation Efficiency*

The absorbed power and radiated power are recorded from the simulation results. The radiation efficiency for the balanced antenna can be calculated using the following formula:

$$\text{efficiency } (\eta) = \frac{P_{\text{radiated}}}{P_{\text{in}} + P_{\text{absorbed}}} \quad (9)$$

The cumulative distribution function (CDF) is evaluated for each location in order to estimate the probability of the power absorbed and radiation efficiency on the human body. Fig. 7 shows the radiation efficiency, and power absorbed values, and their associated CDF evaluated when the mobile placed on these locations. The CDF of the radiated and absorbed power is difficult to predict from the results collected due to the limited sample size generated through the simulation. Recognising the constraints surrounding memory and simulation time, a total of 32 different locations (in line with the rest of the simulation) have been considered, with a view to extrapolating the necessary data. The data from these locations was combined to obtain probability of the efficiency, and can be obtained from Fig. 6. The radiation efficiency values increase as the handset moves from the back to the front of the human body. Hence, these figures clearly indicate that the CDF achieves better radiation efficiency (in the neighbourhood of 40% better) when the mobile been placed on the front of the human model compared to the case of the back position. The reasoning for this appears to be due to a loss of characteristics in the tissue at the front, and a greater degree of absorbed power, as can be seen from the figure.

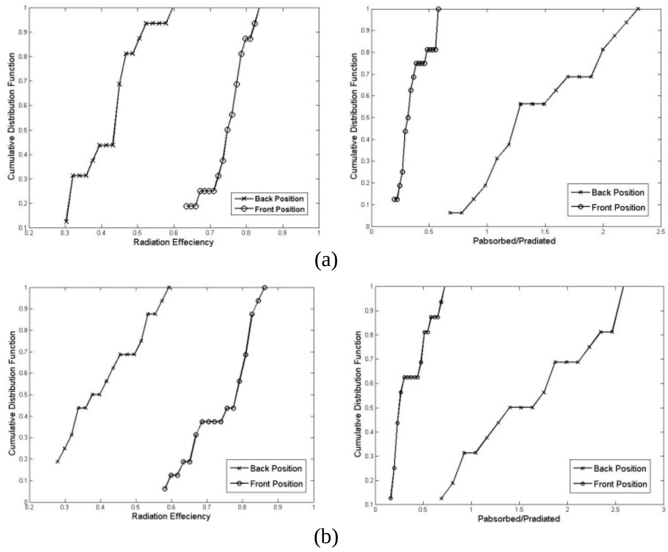

Figure 6: The cumulative distribution function of the radiation effeciency and $P_{absorbed}/P_{radiated}$ when (a)Vertical polarization , (b)Horizantal polarization

In line with our expectations, the figures confirmed that the CDF has similar curves for horizontal and vertical cases for both locations. In addition, it can be reported from Fig. 6 and subsequent calculations, it is evident that standard deviation of the radiation efficiency when the mobile is located in the front is less compared to back location. Taking the previous simulation results into account, we may safely conclude that altering the position of the antenna on the front will not results in a large dispersion in the radiation efficiency. Furthermore the CDF has similar curves for horizontal and vertical cases for both locations.

V. Conclusions

A hybrid MoM/FDTD approach has been adopted for modelling the human body interaction with short range dual band balanced antennas. A total of 32 locations on the human body were investigated, 16 on the back and 16 on the front. In order to ensure the optimal quality of results were achieved through this limited sample, each point was investigated using two polarisations; essentially both horizontal and vertical polarisations. Furthermore, both the far and near fields were incorporated into the study to heighten the understanding of the impact on human tissue both facing the antenna, and not directly facing the antenna. The cumulative distribution function of the radiation efficiency at these locations was also computed. The results support the conclusion that there was a clear improvement in the front compared to the back.

Acknowledgement

The authors would like to thank their colleague Mr.M.B.Child for helpful comments and assistance.

References

[1] K. S. Yee, "Numerical solution of initial boundary value problems involving Maxwell's equations in isotropic media," IEEE Trans on Antennas and Propagation, vol. AP-14, pp. 302-307, 1966.

[2] A. Taflove and S. C. Hagness, Computational electrodynamics: The finite-difference time-domain method, vol. 3rd ed. Boston: MA: Artech House, 2005.

[3] K. S. Kunz and R. J. Luebbers, The finite difference time domain method for electromagnetics, vol. Boca Raton: FL: CRC Press, 1993.

[4] J. P. Berenger, "A perfectly matched layer for the absorption of electromagnetic waves," Journal of Computational Physics, vol. 114, pp. 185-200, 1994.

[5] A. Sani, Y. Zhao, and Y. Hao, "Analysis of on-body propagation channel using a hybrid technique combining the equivalence principle and FDTD," Proceedings of iWAT2008, Chiba, Japan, pp. 502-505, 2008.

[6] M. F. Wong and J. Wiart, "Modelling of electromagnetic wave interactions with the human body," Comptes Rendus Physique, vol. 6, pp. 585-594, 2005.

[7] J. Wang, O. Fujiwara, S. Watanabe, and Y. Yamanaka, "Computation with a parallel FDTD system of human-body effect on electromagnetic absorption for portable telephones," IEEE Transactions on Microwave Theory and Techniques, vol. 52, pp. 53-58, 2004.

[8] O. P. Gandhi and J. Chen, "Numerical dosimetry at power-line frequencies using anatomically based model," Bioelectromagnetics, vol. 13, pp. 43-60, 1992.

[9] K. Fujii, M. Takahashi, K. Ito, and N. Inagaki, "Study on the electric field distributions around whole body model with a wearable device using the human body as a transmission channel," First European Conference on Antennas and Propagation EuCAP pp. 1 - 4, 6-10 Nov. 2006

[10] M. A.-A. Mangoud, "Hybrid Computational Electromagnetics Methods for Personal Communications Applications," in Department of Electronic and Electrical Engineering, vol. PhD Thesis: University of Bradford, 2001.

[11] A. Alhaddad, R. Abd-Alhameed, D. Zhou, C. See, E. Elfergani, M. Bin-Melha, and P. Excell, "New Design of Dual-band Balanced Handset Antenna Design for WLAN Application," In proceeding of Mosharaka International Conference on Communications, Propagation and Electronics (ISBN: 978-9957-486-06-8), vol. Technical Session 1, pp. 1-4, Amman, Jordon, 5-7 March 2010.

[12] NEC-Win Professional V1.1,@1997 Nittany Scientific Inc.,USA.

[13] R. A. Abd-Alhameed, P. S. Excell, and J. Vaul, "Currents Induced on wired I.T. Networks by Randomly distributed phones –A Computational study," IEEE Trans on Electromagnetics and Compatibility, vol. 48, pp. 282-286, May 2006.

[14] P. A. Mason, W. D. Hurt, T. J. Walters, J. A. D'Andrea, K. L. R. P. R. Gajsek, K. I. S. D. A. Nelson, and J. M. Ziriax, "Effects of frequency, permittivity, and voxel size on predicted specific absorption rate values in biological tissue during electromagnetic-field exposure," IEEE Transactions on Microwave Theory and Techniques, vol. 48, pp. 2050 - 2058, Nov 11, 2000.